Mon. Not. R. Astron. Soc. **000**, 000–000 (0000) Printed 15 May 2000 (MN LATEX style file v1.4)

Frequency resolved spectroscopy of Cyg X-1: fast variability of the reflected emission in the soft state.

M. Gilfanov[1,2], E.Churazov[1,2], M. Revnivtsev[2,1]
[1] *Max-Planck-Institute für Astrophysik, Karl-Schwarzschild-Str. 1, 85740 Garching bei München, Germany*
[2] *Space Research Institute, Russian Academy of Sciences, Profsoyuznaya 84/32, 117810 Moscow, Russia,*

15 May 2000

ABSTRACT

Using the RXTE/PCA data we study the fast variability of the reflected emission in the soft spectral state of Cyg X-1 by means of Fourier frequency resolved spectroscopy. We find that the rms amplitude of variations of the reflected emission has the same frequency dependence as the primary radiation down to time scales of $\lesssim 30-50$ msec. This might indicate that the reflected flux reproduces, with nearly flat response, variations of the primary emission. Such behavior differs notably from the hard spectral state, in which variations of the reflected flux are significantly suppressed in comparison with the primary emission, on time scales shorter than $\sim 0.5-1$ sec.

If related to the finite light crossing time of the reflector, these results suggest that the characteristic size of the reflector – presumably an optically thick accretion disk, in the hard spectral state is larger by a factor of $\gtrsim 5-10$ than in the soft spectral state. Modeling the transfer function of the disk, we estimate the inner radius of the accretion disk $R_{in} \sim 100R_g$ in the hard and $R_{in} \lesssim 10R_g$ in the soft state for a $10M_\odot$ black hole.

Key words: accretion, accretion disks – black hole physics – stars: binaries: general – stars: individual (Cygnus X-1) – X-rays: general – X-rays: stars

1 INTRODUCTION

The importance of the reprocessed/reflected component in the X–ray spectra of accreting X–ray sources for exploring the geometry of the accretion flow is well known. Reflection of the primary Comptonized radiation from neutral or partially ionized matter located in the vicinity of the compact object – presumably the optically thick accretion disk, leads to appearance of characteristic features in the spectra of X–ray binaries. The main signatures of the emission reflected from cold neutral medium are well known – the fluorescent K_α line of iron at 6.4 keV, iron K-edge at 7.1 keV and a broad hump at $\sim 20-30$ keV (Basko, Sunyaev & Titarchuk 1974, George & Fabian 1991). The exact shape of these spectral features in the X-ray binaries depends on ionization state of the reflecting medium and might be modified by strong gravity effects and intrinsic motions in the reflector (e.g. Fabian et al., 1989). The amplitude of the reflection signatures depends primarily on the ionization state and the solid angle subtended by the reflector as seen from the source of the primary radiation.

Recently, Revnivtsev, Gilfanov & Churazov (1999, hereafter Paper I) proposed Fourier frequency resolved spectral analysis to study spectral variability in the X-ray binaries. Although interpretation of the Fourier frequency resolved spectra in general is not straightforward and requires a priori assumptions to be made, one of the areas where this method can be efficiently used is the fast variability of the reflected component. It has been found that in the low spectral state of Cyg X-1 and GX339-4 the energy spectra corresponding to the shorter time scales ($\lesssim 0.1-1$ sec) show less reflection than those of longer time scales (Revnivtsev, Gilfanov & Churazov 1999, 2000). The simplest, although not unique, interpretation of this result is smearing of the short term variations of the reflected emission due to finite light crossing time of the reflector. Based on the Fourier frequency dependence of the equivalent width of the Fe K_α fluorescent line Revnivtsev et al. (1999) estimated the characteristic size of the reflector: $\sim 80-160R_g$ for a $20-10M_\odot$ black hole.

In this paper we investigate the fast variability of the reflected component in the soft spectral state of Cyg X-1 and compare it with that in the hard spectral state.

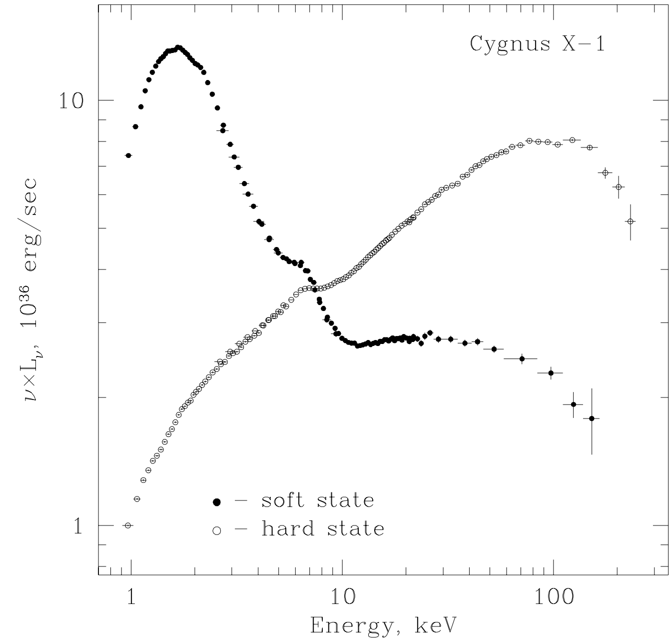

Figure 1. The spectral energy distribution of Cyg X–1 in the soft (filled circles) and hard (open circles) spectral state. The data of nearly simultaneous ASCA and RXTE observations on March 26, 1996 (hard state) and May 30, 1996 (soft state). A source distance of 2 kpc was assumed (Gierlinski et al. 1999).

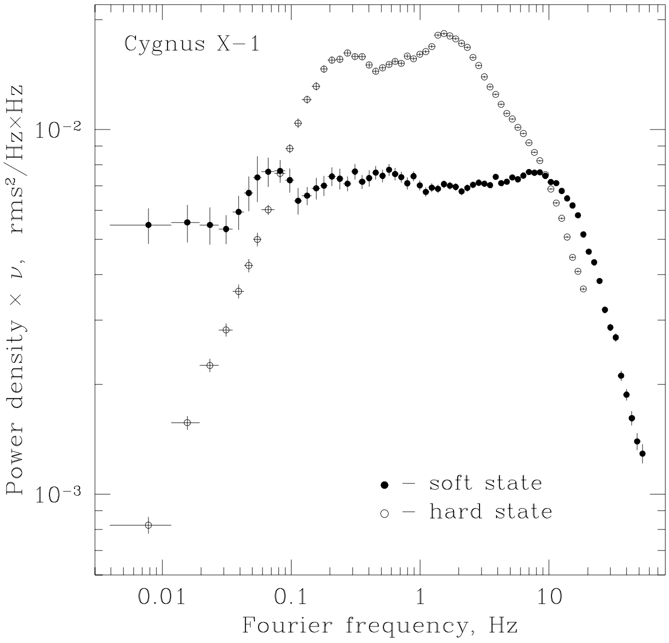

Figure 2. The power density spectra of Cyg X–1 in the soft (filled circles) and hard (open circles) spectral state in the 3–13 keV energy band. The power spectra are plotted as (power density) × frequency, i.e. in units of $rms^2/Hz \times Hz$ and are cut at approximately half of the Nyquist frequency (32 and 128 Hz for the hard and soft state respectively). No correction for binning and aliasing effects has been applied.

2 OBSERVATIONS AND DATA ANALYSIS.

We used publicly available data of Cyg X–1 observations with the Proportional Counter Array aboard the Rossi X-ray Timing Explorer (Brandt Rotschild & Swank 1996) performed in June, 1996 during the soft spectral state of the source. The list of the observations is given in Table 1. The total live time was ≈ 11.5 ksec. The "Generic Binned" mode data in configuration B_4ms_8A_0_35_H, with time resolution of ≈ 4 msec and covering 2.9-13.1 keV energy range was used for frequency resolved spectral analysis.

The data screening and selection was performed using FTOOLS 4.2 with standard screening criteria recommended by RXTE GOF. The frequency resolved spectra were calculated following the prescription detailed in Paper I. The dead time corrected value of the white noise level was determined from fitting of the power spectra in the 300-1000 Hz frequency range. The spectral analysis was performed in XSPEC v.10.0 (Arnaud 1996) with version 3.5 of the PCA response matrix. A uniform systematic error of 0.5% was added quadratically to the statistical error in each energy channel.

The observations of the source during the hard state discussed in the text were performed between March 26 and 31, 1996. The details of these observations are given in Paper I.

Table 1. The list of RXTE observations used for the analysis.

Obs.ID	Date (UT)	Start	End	Expos.,s*
10512-01-05-00	04/06/96	20:49:36	21:43:44	1249
10512-01-07-00	16/06/96	00:07:44	00:21:04	643
10512-01-07-02	16/06/96	04:55:44	05:17:04	1113
10512-01-08-01	17/06/96	01:44:32	01:56:00	532
10512-01-08-02	17/06/96	04:56:32	05:17:52	1081
10512-01-08-00	17/06/96	08:08:32	08:44:00	1871
10512-01-09-02	18/06/96	03:21:36	03:36:00	675
10512-01-09-00	18/06/96	06:34:40	07:01:52	1461
10512-01-09-01	18/06/96	09:46:40	10:26:56	2170

* Dead time corrected PCA exposure time.

3 RESULTS.

The broad band energy spectra of Cyg X-1 in the hard and soft spectral state are shown in Fig.1. The spectra were obtained using the data of overlapping ASCA and RXTE observations of the source on March 26, 1996 (hard state) and on May 30, 1996 (beginning of the soft state).

The power spectra of Cyg X-1 in the 3–13 keV energy band in the hard and soft spectral states obtained from the complete sets of the data used for the frequency resolved spectral analysis in this paper and in Paper I are shown in Fig.2. The power density is plotted in units of power×frequency representing squared fractional rms at a given frequency per factor $\sim e$ in frequency. This way of representing the power spectra most clearly characterizes relative contribution of variations at different frequencies to the total observed rms.

The Fourier frequency resolved spectra for the soft spectral state were obtained in 10 frequency bins of logarithmi-

Table 2. Dependence of the best fit parameters upon Fourier frequency

Frequency range, Hz	*soft state* phot.ind. Γ^1	EW^2, eV	EW/EW($<$ 1Hz)^3	*hard state* phot.ind. Γ^1	EW^2, eV	EW/EW($<$ 1Hz)^3
0.016–0.078	2.60 ± 0.032	494 ± 83	1.05 ± 0.18	1.97 ± 0.006	145 ± 16.6	0.97 ± 0.11
0.078–0.20	2.60 ± 0.022	484 ± 61	1.03 ± 0.13	1.95 ± 0.004	153 ± 13.0	1.02 ± 0.09
0.20–0.45	2.63 ± 0.018	482 ± 48	1.02 ± 0.10	1.94 ± 0.004	152 ± 11.3	1.02 ± 0.08
0.45–1.0	2.62 ± 0.014	424 ± 38	0.90 ± 0.08	1.94 ± 0.004	149 ± 10.4	1.00 ± 0.07
1–2	2.63 ± 0.012	445 ± 33	0.94 ± 0.07	1.89 ± 0.004	121 ± 9.8	0.81 ± 0.07
2–4	2.64 ± 0.011	429 ± 31	0.91 ± 0.07	1.86 ± 0.004	121 ± 9.9	0.81 ± 0.07
4–8	2.64 ± 0.011	413 ± 31	0.88 ± 0.07	1.81 ± 0.004	107 ± 11.4	0.71 ± 0.08
8–16	2.58 ± 0.011	462 ± 35	0.98 ± 0.07	1.70 ± 0.007	75 ± 16.6	0.50 ± 0.11
16–32	2.52 ± 0.018	410 ± 59	0.87 ± 0.13	1.69 ± 0.017	47 ± 37.8	0.31 ± 0.25
32–128	2.43 ± 0.050	233 ± 172	0.49 ± 0.37	––	––	––

The errors are 1σ for one parameter of interest.
[1] – the power law photon index;
[2] – the equivalent width of the 6.4 keV line, eV;
[3] – EW($<$ 1Hz) – equivalent width averaged in the 0.016-1.0 Hz frequency range

cally equal width in the 0.016-128 Hz frequency range. In order to study the frequency dependence of the amplitude of the reflected component we fit the spectra in the 3–13 keV band with a simplified model consisting of an absorbed power law* with superimposed Gaussian line at 6.4 keV. The low energy absorption was fixed at $N_H = 6 \cdot 10^{21}$ cm^{-1}. The line width (standard deviation for a Gaussian profile) was fixed at 1 keV which corresponds to the average value for the high state observations used for the analysis. The power law photon index and line flux were the only free parameters of the fit. To facilitate comparison with the hard state data we reanalyzed the data set used in Paper I in identical frequency bins covering 0.016-32 Hz frequency range (the time resolution of the hard state data was ≈ 16 msec) and using the same spectral model. The width of the line for the hard state spectra was fixed at the corresponding average value of 0.8 keV (Gilfanov, Churazov & Revnivtsev 1999).

Such a spectral model is obviously oversimplified. Neither it is justified from the physical point of view. In particular it might lead to a certain overestimate of the equivalent width of the line since the line tends to include a fraction of the reflected continuum photons. It is, however, suitable to quantify the amplitude of the characteristic "wiggle" usually seen in the spectra of the accreting X–ray sources in the $\sim 5-15$ keV energy range and commonly attributed to the effects of reflection. Use of more sophisticated models is restricted by insufficient statistics (especially in the soft spectral state) and the low number of energy channels below ≈ 13 keV in the B_4ms_8A_0_35_H configuration used in the most of the soft state observations.

The best fit values of the spectral parameters for both spectral states are given in Table 2. The dependence of the equivalent width on the Fourier frequency is shown in Fig.3. Variations of the parameters of the spectral model, in particular the change of the line centroid from 6.0 to 6.7 keV and reducing the intrinsic line width to zero, do not change the general trend. These variations, however, affect the particular values of the equivalent width and, to lesser extent, the shape of the curve in Fig. 3.

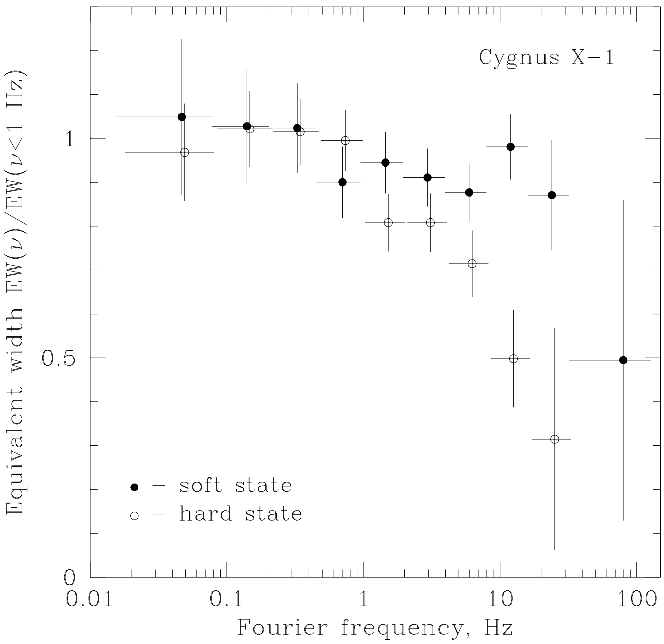

Figure 3. Equivalent width of the Fe fluorescent line vs. Fourier frequency in the soft (filled circles) and hard (open circles) spectral state. The equivalent width is normalized to the 0.01-1 Hz average.

According to the χ^2–test two distributions, shown in Fig.3 differ at the confidence of level of $\approx 98.7\%$ ($\chi^2 = 19.4$ for 8 d.o.f. in the 0.016–32 Hz frequency range). It should be noted, however, that the error bars assigned to the Fourier frequency resolved spectra were propagated from the corresponding power density spectra and are likely to be somewhat overestimated, especially in the low frequency bins (this fact can be noticed in Fig.3). The confidence level,

* Contrary to the average spectra of Cyg X-1 in the soft state (Fig.1), the contribution of the soft component to the frequency resolved spectra is negligible (to be discussed in more detail in a separate paper). Therefore use of a power law to model continuum emission in the soft state is justified.

calculated using 0.45–32 Hz frequency range is $\approx$ 99.7% ($\chi^2 = 18.1$ for 5 d.o.f.).

4 FREQUENCY DEPENDENCE OF THE EQUIVALENT WIDTH AND TIME RESPONSE OF THE REFLECTOR.

We assume below that the spectrum of the primary radiation and the geometry, element abundances and ionization state of the reflector are fixed. The equivalent width of the Fe fluorescent line determined from a conventional energy spectrum is proportional to the relative amplitude of the reflected component and approximately measures the solid angle subtended by the reflector. The equivalent width of the fluorescent line determined from a Fourier frequency resolved spectrum measures the ratio of the rms amplitudes of variations of the reflected component and the primary emission in a given Fourier frequency range. The constancy of the equivalent width of the line at Fourier frequencies $f \lesssim 30$ Hz observed in the soft state (Fig.3) implies that the rms amplitude of variations of the reflected component has the same frequency dependence as that of the primary radiation. This would naturally appear if the reflected emission was reproducing variations of the primary radiation down to the time scales of $\sim 30-50$ msec. Such behavior is in contrast to the hard spectral state, in which variations of the reflected flux are notably suppressed in comparison with the primary emission on the time scales shorter than ~ 500 msec.

The most straightforward explanation of this effect would be in terms of a finite light crossing time of the reflector $\tau_{\rm refl} \sim l_{\rm refl}/c$ due to its finite spatial extend $l_{\rm refl}$. In this case the frequency dependence of the fluorescent line equivalent width, $EW(f)$, is determined by the geometry of the primary source and the reflector. The characteristic width of the $EW(f)$ is mainly defined by the spatial extent of the part of the accretion disk giving the main contribution to the reflected emission. Based on these arguments Revnivtsev, Gilfanov & Churazov (1999) estimated the characteristic size of the reflector in the low spectral state as $l_{\rm refl} \sim 5\times10^8$ cm which would correspond to $\sim 150R_{\rm g}$ for a $10M_\odot$ black hole.

Various aspects of reverberation of the primary radiation by an accretion disk have been studied by many authors (e.g. Matt & Perola 1992, Campana & Stella 1995). Below we consider this problem in the context of Fourier frequency resolved analysis. The time dependence of the reflected emission is defined by the following relation:

$$F_{refl}(t) = \int_0^\infty F_0(t-\tau)T(\tau)d\tau$$

where $F_0(t)$ and $F_{refl}(t)$ are primary and reflected flux, $T(\tau)$ – the transfer function of the reflector, defined by the geometry. This function accounts for the propagation time of the photons from the primary source to different parts of the reflector and then to the observer. The Fourier transform of the reflected flux is:

$$\hat{F}_{refl}(f) = \hat{F}_0(f)\times\hat{T}(f)$$

where $\hat{F}_0$, $\hat{F}_{refl}$ and $\hat{T}$ are corresponding Fourier transforms and f is Fourier frequency. The equivalent width of the fluorescent line determined from the Fourier frequency resolved spectra is

$$EW(f) \propto \frac{|\hat{F}_{refl}(f)|}{|\hat{F}_0(f)|} = |\hat{T}(f)|$$

i.e. is proportional to the Fourier transform of the transfer function of the reflector.

Fig.4 shows the transfer function and its Fourier transform for an isotropic point source located at the height h above a flat disk with the inner radius R_{in} and inclination angle i for different values of R_{in} and i. A Lambert law for the angular dependence of the reflected flux has been assumed. No general or special relativity effects have been taken into account. The characteristic width of the $EW(f)$ dependence is mainly defined by the distance $d = \sqrt{h^2+R_{in}^2}$ between the primary source and the inner edge of the disk and depends only weakly on the inclination angle i. A small offset of the primary source, $\Delta \ll d$ or non-zero opening angle of the disk do not significantly affect the characteristic width of Fourier transform of the response function (Fig.5). However, the transfer function itself and the high frequency part of its Fourier transform are sensitive to the details of the geometry (Fig. 4 and 5).

In Fig.6 we compare Fourier transform of the transfer function of a flat disk with inclination $i = 50^\circ$, appropriate for Cyg X-1 (Gies & Bolton 1986), with the frequency dependence of the equivalent width observed in the soft and hard spectral states of Cyg X-1. As seen from Fig.6, suppression of the high frequency variations in the reflected emission observed in the hard state can be satisfactorily described by reflection from a disk with an inner radius of $R_{in} \sim 100R_g$ around a $10M_\odot$ black hole. Significantly larger, $R_{in} \sim 1000R_g$, or smaller values of the inner radius, $R_{in} \sim 10R_g$, are inconsistent with the data. The soft state data, on the other hand, requires much smaller values of the inner radius of the disk, $R_{in} \sim 10R_g$.

It should be noted that since we use the equivalent width of the Fe fluorescent line as a measure of the amplitude of the reflected emission, the results might be somewhat affected by the non-uniformity of the ionization state of the accretion disk with radius and geometrical effects (e.g. radial and azimuthal dependence of the reflection angle). Results of more detailed modeling of the disk transfer function and rigorous comparison with the data will be published elsewhere (a paper in preparation).

5 DISCUSSION.

Study of fast variability of the reflected emission by means of Fourier frequency resolved spectroscopy offers a new independent method to probe the geometry of the accretion flow which complements conventional X-ray spectral analysis. The presence of a luminous soft component dominating the X-ray spectrum in the soft spectral state of black hole candidates (Fig.1) strongly favors small values of the inner radius of the disk (e.g. Gierlinski et al., 1999), in good agreement with the above result, $R_{in} \lesssim 10R_g$. In the hard spectral state conventional estimates of the inner radius of the accretion disk range from several tens R_g in coronal model (e.g. Poutanen, Krolik & Ryde, 1997; Done & Zycki, 1999) to several hundred R_g in ADAF model (e.g. Esin et al., 1998). Our result, $R_{in} \sim 100R_g$, falls in the middle of this range.

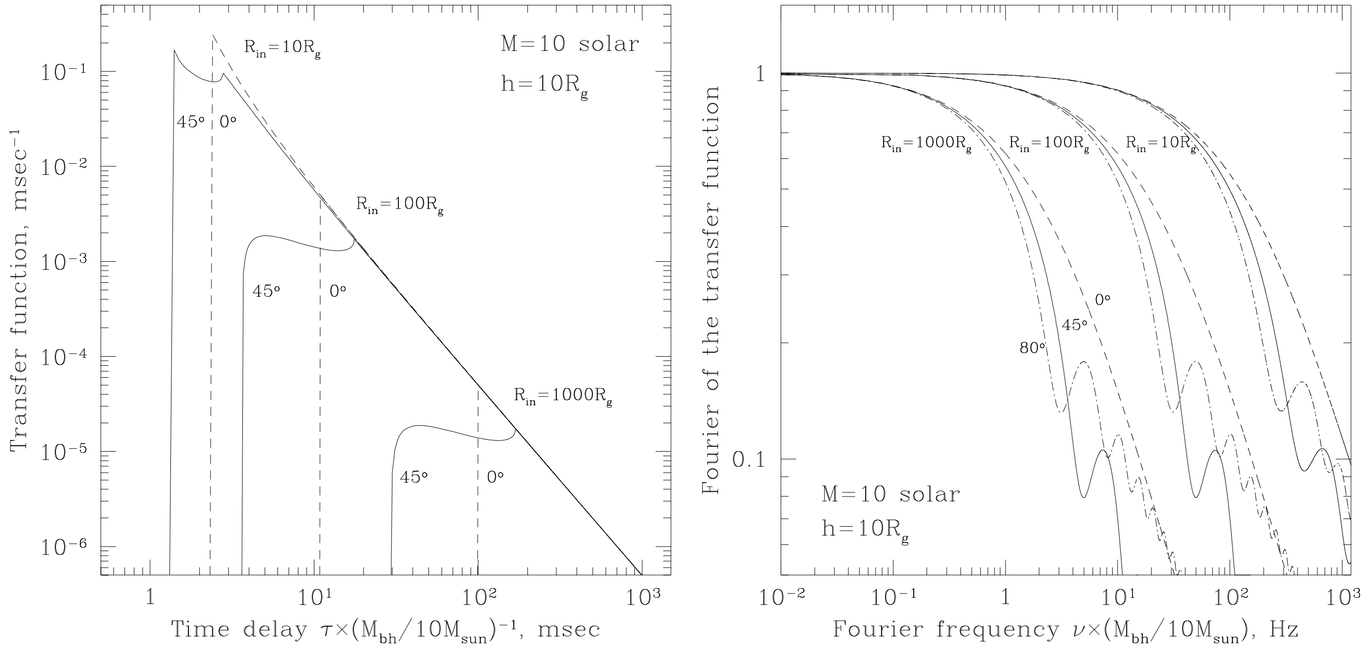

Figure 4. Transfer function (*left*) of the disk and its Fourier transform (*right*) for an isotropic point source of primary radiation located at $h = 10R_g$ above a flat disk with inner radius of $R_{in} = 10, 100$ and $1000R_g$ and inclination angle of $0°, 45°$ and $80°$ (not shown in the left panel). No relativistic effects have been taken into account. The linear quantities are given in the units of gravitational radii $R_g = 2GM/c^2$ for a $10M_\odot$ black hole. The normalization of the transfer function is arbitrary.

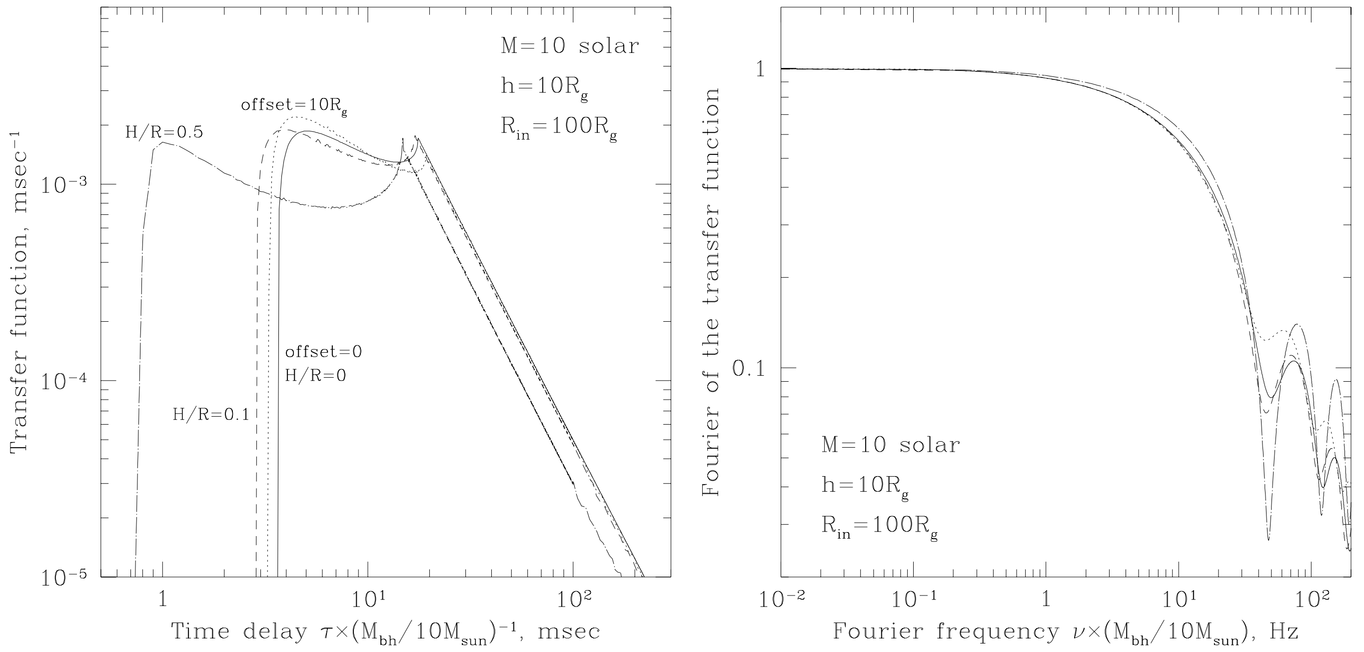

Figure 5. Dependence of the transfer function and its Fourier transform upon offset of the source of the primary radiation from the disk axis (offset=$10R_g$, flat disk – dotted line) and opening angle of the disk (offset=0, $H/R = 0.1$ – dashed line and $H/R = 0.5$ – dash-dotted line). Other parameters of the model are: inner disk radius $R_{in} = 100R_g$, $M = 10M_\odot$, inclination 45°. No relativistic effects have been taken into account. The linear quantities are given in the units of gravitational radii $R_g = 2GM/c^2$ for a $10M_\odot$ black hole.

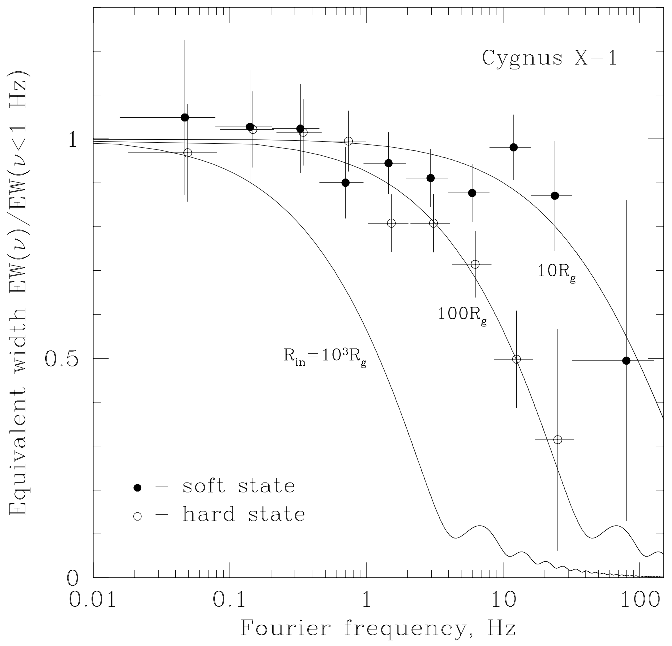

Figure 6. Equivalent width of the Fe fluorescent line vs. Fourier frequency. Comparison of the data with the model. The data points are the same as in Fig.3. The model curves were calculated for an isotropic point source at height $h = 10R_g$ on the axis of a flat disk with inner radius of $10, 100$ and $1000R_g$ (assuming a $10M_\odot$ black hole) and with inclination angle of $50°$.

The inner radius of the accretion disk determined in the above analysis refers to the inner radius of the "reflective" part of the disk, where the ionization state is such that the disk is capable to produce a fluorescent iron line. Therefore substantial change of the ionization state of the surface layer of the inner disk in the course of a spectral state transition (e.g. Young et al., 1999) may have similar effect on the frequency dependence of the equivalent width of the iron line as physical change of the inner disk radius.

Considering the transfer function formalism in the previous section we assumed that the shape of the spectrum of the primary radiation, geometry and ionization state of the reflector did not change during the course of flux variations. The assumption of the constant primary spectrum seems to be correct for the soft state as there is no significant frequency dependence of the Fourier resolved spectra (Table 2). In the hard state, on the contrary, the flux variations are accompanied with a notable spectral variability. The effect, however, should not be strong due to moderate dependence of the equivalent width on the slope of the incident spectrum – $\Delta\Gamma = \pm 0.2$ at $\Gamma_0 = 1.7$ causes a $\mp 10\%$ change in the equivalent width (George & Fabian 1991), which is significantly smaller than that expected due to the flux variations. Moreover, for the type of spectral variability observed in the hard state this would flatten the $EW(f)$ dependence strengthening the conclusion about the fall off at the high frequencies. Short term variations of the ionization state of the disk is another factor that can affect the equivalent width of the line in the frequency resolved spectra. Its effect is however negligible for ionization parameters less than a few hundred (Matt, Fabian & Ross 1993) which is probably the case in the hard state (Done & Zycki 1999). Ionization parameter is less constrained but is likely to be higher in the soft state (Gierlinski et al. 1999). However, constancy of the the Fourier resolved spectra with frequency (Table 2) and significantly suppressed short-term variability of the soft component (Gilfanov, Churazov, Revnivtsev 2000 in preparation) hints at absence of significant short term variations of the ionization state of the disk. To conclude, the above effects might affect somewhat the estimates of the characteristic size of the reflector, especially in the hard state, but they should not change the qualitative conclusion that it is notably large in the hard state than in the soft state.

In the simplified geometry of an isotropic point source above flat disk solid angle subtended by the reflector is $\frac{\Omega}{2\pi} = \frac{1}{\sqrt{1+R_{in}^2/h^2}}$ (in the notation of the previous section). For the parameters from Fig.6 respective values of the solid angle are: $\frac{\Omega}{2\pi} \approx 0.1$ for the hard state ($h = 10R_g$, $R_{in} = 100R_g$) and $\frac{\Omega}{2\pi} \approx 0.7$ for the soft state ($h = 10R_g$, $R_{in} = 10R_g$). Equivalent width of the iron fluorescent line expected for these values of the solid angle and solar abundance of iron are several times smaller than those given in the Table 2, especially for the hard spectral state. However, as was noted above, the absolute values of the equivalent width quoted in Table 2 are subject to some uncertainty and can be overestimated due to simplified model used for the spectral fits. Comparison of the model predictions with more accurately determined values of the equivalent width and amplitude of the reflected component can further constrain geometry of the accretion flow.

Finally, we should note that interpretation of the frequency dependence of the equivalent width of the fluorescent line in terms of the finite light crossing time of the reflector is not unique. An alternative explanation might be that the short time scale, $\lesssim 50$–100 msec, variations appear in a geometrically different, likely inner, part of the accretion flow and give a rise to significantly weaker, if any, reflected emission than the longer time scale events presumably originating in the outer regions. This might be caused, for instance, by a smaller solid angle of the reflector as seen by the short time scale events and/or due to screening of the reflector from the short time scale events by the outer parts of the accretion flow. However, independent of the nature of the fall off of the equivalent width at high frequency, the flat response of the reflected emission to variations of the primary radiation observed at low frequencies puts an upper limit on the spatial extent of the reflector, i.e. on the inner radius of the accretion disk. In particular, large values of R_{in}, significantly exceeding $\sim 100R_g$ in the hard and $\sim 10R_g$ in the soft spectral state are excluded by our analysis.

6 CONCLUSIONS.

We have exploited Fourier frequency–resolved spectral analysis to study fast variability of the reflected emission on time scales of ~ 100 sec – 10 msec in the soft and hard spectral states of Cyg X-1. Our conclusions are:

(i) In the soft spectral state variations of the reflected component have the same frequency dependence of the rms amplitude as the primary emission up to the frequencies $\gtrsim$ 30 Hz. This would be expected if, for instance, the reflected flux was reproducing, with flat response, variations of the primary radiation down to the time scales of $\sim 30 - 50$ msec. The sensitivity of the present analysis is insufficient to study shorter time scales.

(ii) In the hard spectral state variability of the reflected flux is significantly suppressed in comparison with the direct emission on the time scales shorter than $\sim 0.5 - 1$ sec (see also Paper I).

(iii) Assuming that suppression of the short-term variability of the reflected emission is caused by the finite light-crossing time of the reflector, we estimated the inner radius of the accretion disk $R_{in} \sim 100 R_g$ in the hard spectral state and $R_{in} \lesssim 10 R_g$ in the soft spectral state.

ACKNOWLEDGMENTS

This research has made use of data obtained through the High Energy Astrophysics Science Archive Research Center Online Service, provided by the NASA/Goddard Space Flight Center. The authors thank the referee, Chris Done, for useful comments. The work was done in the context of the research network "Accretion onto black holes, compact objects and protostars" (TMR Grant ERB-FMRX-CT98-0195 of the European Commission). M.Revnivtsev acknowledges partial support by RBRF grant 97-02-16264 and INTAS grant 93–3364–ext.

REFERENCES

Arnaud, K.A., 1996, Astronomical Data Analysis Software and Systems V, eds. Jacoby G. and Barnes J., p17, ASP Conf. Series volume 101.
Basko M., Sunyaev R. & Titarchuk L., 1974, A&A, 31, 249
Brandt, H., Rotschild, R. & Swank, J. 1996, Memorie della Societa Astronomica Italiana, 67, 593
Campana S., Stella L., 1995, MNRAS, 272, 585
Done C., Zycki P., 1999, MNRAS, 305, 457
Esin A.A. et al., 1998, ApJ, 505, 854
Fabian et al. 1989, MNRAS, 238, 729
George I.M., Fabian A.C., 1991,
Gierlinski M. et al., 1999, MNRAS, 309, 496
Gies D. & Bolton C., 1986, ApJ, 304, 371
Gilfanov M., Churazov E. & Revnivtsev M., 1999, A&A, 352, 182
Matt G. , Perola G.C., 1992, MNRAS, 259, 433
Matt G., Fabian, A. C., Ross R.R., 1993, MNRAS, 262, 179
Poutanen J., Krolik J.H. & Ryde F., 1997, MNRAS, 292, L21
Revnivtsev M., Gilfanov M. & Churazov E., 1999, A&A Letters, 347, L23 (Paper I)
Revnivtsev M., Gilfanov M. & Churazov E., 1999, A&A Letters, submitted
Young, A. J., Fabian, A. C., Tanaka, Y. & Ross, R. R. 1999, American Astronomical Society Meeting, 195, 112604